Epitrochoids and Hypotrochoids Together Again

Greg Dresden

Greg Dresden (dresdeng@wlu.edu) is a professor of mathematics at Washington & Lee University in the mountains of Virginia. He received his PhD from the University of Texas a great many years ago. He was a living kidney donor in 2018 and he encourages everyone to learn more about this gift of life.

The idea for this article came from a recent problem in the *College Mathematics Journal* which asked for the area of one of the four inner loops in the following picture.

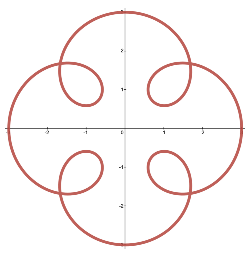

Figure 1. An epitrochoid with four-fold symmetry.

This particular figure is called an *epitrochoid* [**2, 3**] and according to Lawrence [**3**] it dates back to Alfred Dürer's work in 1525. It is described by the parametric equations

$$\begin{aligned} x(t) &= 2\cos t + \cos 5t, \\ y(t) &= 2\sin t + \sin 5t. \end{aligned} \tag{1}$$

An obvious question is why Figure 1 has four-fold symmetry despite the presence of the terms $\cos 5t$ and $\sin 5t$ in equations (1). To answer this question, we need to rewrite the above pair of equations as a single complex-valued equation. If we let $x(t)$ and $y(t)$ be the real and imaginary part, respectively, of $z(t)$, and if we make use of Euler's identity $e^{i\theta} = \cos\theta + i\sin\theta$, then equations (1) become

$$z(t) = x(t) + iy(t) = 2e^{it} + e^{5it} = e^{it}\left(2 + e^{4it}\right), \tag{2}$$

and now the four-fold symmetry is revealed. To be precise, we note that since equation (2) tells us that $z(t) = e^{it}(2 + e^{4it})$, then

$$z(t + \pi/2) = e^{i\pi/2} z(t),$$

which tells us that $z(t+\pi/2)$ has the same modulus as $z(t)$ and is rotated 90° counterclockwise on the complex plane. See Farris [**1**, Ch. 3] and Mutalik [**4**] for more examples of this kind of symmetry argument.

We can see that moving to *complex* variables actually *simplifies* the situation (if you'll forgive the atrocious pun). This does lead to another question: what other discoveries can we make by writing parametric curves in terms of complex variables?

An imperfect nesting To generate a second curve, we decide to make the simplest possible change to equation (2): we replace the e^{4it} with e^{-4it}, giving us the new equation

$$z(t) = e^{it}\left(2 + e^{-4it}\right). \tag{3}$$

When we convert back to Cartesian coordinates, we get a new set of equations,

$$\begin{aligned} x(t) &= 2\cos t + \cos 3t, \\ y(t) &= 2\sin t - \sin 3t, \end{aligned} \tag{4}$$

and this now describes a figure called a *hypotrochoid* [**2, 3**]. Figure 2 shows the hypotrochoid from equations (4) in blue, nested together with the epitrochoid from equations (1) in red.

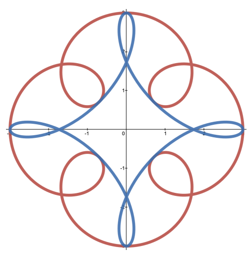

Figure 2. A not-quite-perfect nesting of a red epitrochoid and blue hypotrochoid.

From looking at the complex-variable equations $e^{it}\left(2+e^{4it}\right)$ for the earlier epitrochoid and $e^{it}\left(2+e^{-4it}\right)$ for the current hypotrochoid, we can see that not only do both have four-fold symmetry but also they clearly intersect each other when the parameter t is a multiple of $\pi/4$, thanks to the convenient fact that $e^{i\pi} = e^{-i\pi}$. Coincidentally, these intersections are when the polar angle θ is a multiple of $\pi/4$, and this explains why the two curves are nested together as seen in Figure 2. These intersections are also at the maximal modulus and minimal modulus (3 and 1, respectively) for the two complex-variable equations. As we will show later, we can even improve this nesting by slightly altering the graphs.

Epitrochoids and hypotrochoids are often *discussed* together, as they are both formed by taking a point attached to the radius of one circle that is rolling around the circumference of a second circle. However, we have not seen them actually *drawn* together as in Figure 2 above and Figures 4 and 5 below. Thanks to our decision to work with complex variables, it was the similarities between equations (2) and (3) that led to our decision to draw them together (as in Figure 2 above) and subsequently led to the other discoveries in this article.

But first, a warning about a common pitfall when talking about complex-variable parametric equations.

 © THE MATHEMATICAL ASSOCIATION OF AMERICA

The parameter is not always polar It might be tempting to think of the parameter t as measuring the polar angle θ of the point $(x(t), y(t))$ on the Cartesian plane. While the epitrochoid and hypotrochoid from Figure 2 do indeed intersect each other at the polar angle $\theta = 0$ when $t = 0$ (and likewise at θ and t equal to multiples of $\pi/4$ as mentioned above), this is not the case in general. In fact, as the parameter t increases slightly from $t = 0$, the polar angle θ for the point on the hypotrochoid actually *decreases* from $\theta = 0$ before then increasing. We can see this by tracing out the path of the point $(x(t), y(t))$ for the hyptrochoid given by equations (4) as t increases from $t = 0$ in multiples of $\pi/12$, as shown here in Figure 3. Note that at $t = \pi/12$ the polar angle θ is slightly negative, and at $t = 2\pi/12$ we have $\theta = 0$. Clearly, t and θ are not always the same.

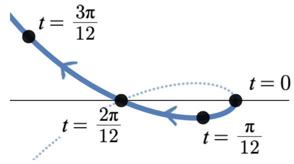

Figure 3. Path of hypotrochoid for small values of t.

A perfect nesting If we move from four-fold to six-fold symmetry by using the equations $z(t) = e^{it}\,(2 + e^{6it})$ and $z(t) = e^{it}\,(2 + e^{-6it})$, we might be surprised at how well the two graphs fit together.

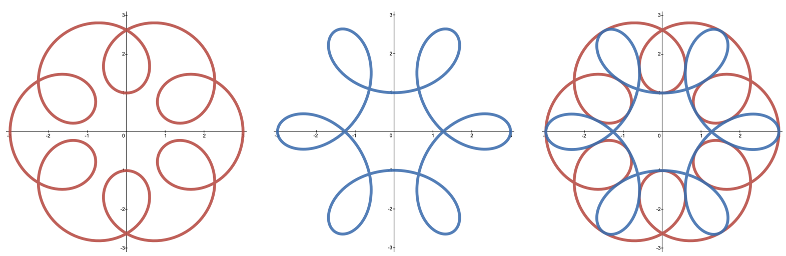

Figure 4. Best possible nesting.

On the left of Figure 4 we have the epitrochoid in red with six-fold symmetry, and in the middle is the corresponding six-fold hypotrochoid in blue. On the right we can see how they fit together perfectly; not only do they intersect and are tangent at the six "inside" and the six "outside" points at radius 1 and 3 respectively, but also they intersect and are tangent at the twelve "middle" points, each at radius $\sqrt{3}$. There are, in all, 24 points of tangency. (See Figure 6 for clarity.)

As we will now show, we can also achieve this kind of perfect nesting for the four-fold symmetric figures, and in fact for k-fold symmetry for all values of $k > 2$. All we have to do is modify our equations just a little bit.

A more perfect nesting

For context, we show in Figure 5 the best possible nestings for the four, six, and thirteen-fold symmetric epitrochoids and hypotrochoids. The epitrochoids are in solid red, and the hypotrochoids in dashed blue. The scale is the same in all three.

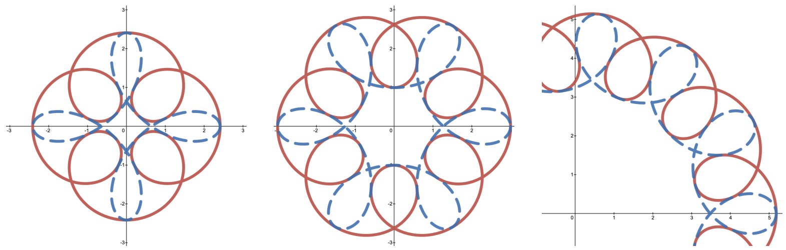

Figure 5. More perfect nestings for $k = 4, 6$, and 13.

We say this is a *perfect nesting* when the epitrochoid and hypotrochoid of k-fold symmetry are tangent at k points of intersection on the inside, $2k$ points of intersection in the middle, and k points of intersection on the outside. See Figure 6.

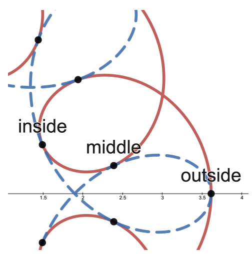

Figure 6. Points of intersection and tangency.

We mentioned earlier that we can achieve perfect nesting if we "... modify our equations just a little bit". As the following theorem shows, we simply need to modify the 2 in equations (1) and (4) to a new value that is dependent on k.

Theorem 1 (Nesting Theorem). *For the epitrochoid $(x_e(t), y_e(t))$ and hypotrochoid $(x_h(t), y_h(t))$ of k-fold symmetry defined as*

$$x_e(t) = A_k \cos t + \cos(k+1)t, \qquad x_h(t) = A_k \cos t + \cos(k-1)t,$$
$$y_e(t) = A_k \sin t + \sin(k+1)t, \qquad y_h(t) = A_k \sin t - \sin(k-1)t,$$

with $k > 2$, then we have perfect nesting when $A_k = \csc \pi/k$. Furthermore, the radii of intersections are $\csc \pi/k - 1$ and $\csc \pi/k + 1$ for the inside and outside points, and $\cot \pi/k$ for the middle points.

As an example, we note that for $k = 6$ then this theorem tells us that $A_6 = \csc \pi/6 = 2$, which gives us the perfect nesting in Figure 4, and it tells us that the radii of intersections are $\csc \pi/6 - 1, \csc \pi/6 + 1$, and $\cot \pi/6$ which give us the values $1, 3$, and $\sqrt{3}$ as mentioned earlier.

 © THE MATHEMATICAL ASSOCIATION OF AMERICA

Likewise, for $k = 4$ the epitrochoid and hypotrochoid in equations (1) and (4) as seen in Figure 2 do not have perfect nesting. To achieve the perfect nesting, we would simply need to replace the 2 in equations (1) and (4) with $A_4 = \csc \pi/4 = \sqrt{2}$; the result is seen in the picture on the left of Figure 5.

Proof of Theorem 1. As mentioned earlier, there are inherent advantages in writing our Cartesian equations in terms of complex variables. In doing this for the equations in the statement of Theorem 1, we get

$$z_e(t) = e^{it}\left(A_k + e^{ikt}\right) \qquad \text{and} \qquad z_h(t) = e^{it}\left(A_k + e^{-ikt}\right) \tag{5}$$

for the epitrochoid and hypotrochoid, respectively. We can now see that both curves have k-fold rotational symmetry since

$$z_e(t + 2\pi/k) = e^{i2\pi/k} z_e(t) \qquad \text{and} \qquad z_h(t + 2\pi/k) = e^{i2\pi/k} z_h(t), \tag{6}$$

telling us that when we increase t by $2\pi/k$ we get a point with the same modulus but rotated $2\pi/k$ counterclockwise.

At this point, we could simply study a sector of angular width $2\pi/k$ and then appeal to the k-fold symmetry. However, we can do a bit more. Since

$$z_e(-t) = \overline{z_e(t)} \qquad \text{and} \qquad z_h(-t) = \overline{z_h(t)}, \tag{7}$$

then both graphs are symmetric across the x-axis as well. This means that we need only focus our attention on the sector in the first quadrant from the horizontal axis to the ray at polar angle $\theta = \pi/k$ measured counterclockwise from the horizontal. By symmetry above/below the x-axis, we can copy this below the x axis (giving us a sector from angle $-\pi/k$ up to π/k) and then from our k-fold symmetry we can multiply this sector by k to give us the entire shape. See Figure 7 for an illustration.

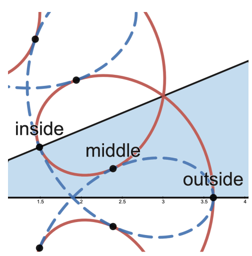

Figure 7. By symmetry, we need only consider this one sector from $\theta = 0$ to $\theta = \pi/k$.

With this in mind, we start by showing that the two curves do indeed intersect at the outside and inside points by noting that

$$z_e(0) = A_k + 1 = z_h(0)$$

and

$$z_e(\pi/k) = e^{i\pi/k}(A_k - 1) = z_h(\pi/k).$$

The moduli of these complex numbers above are $A_k + 1$ and $A_k - 1$, giving us the outside and inside radii of intersection as mentioned in the theorem. Since these are the maximum and minimum values, respectively, for the moduli of the two curves, then we know that both curves are in fact tangent to the circle of radius $A_k + 1$ (on the outside) or $A_k - 1$ (on the inside) at those points of intersection and hence are tangent to each other.

We now turn our attention to the middle points of intersection, as seen in Figure 7. Here, things are a little bit more difficult because the epitrochoid and hypotrochoid actually "intersect" at that middle point at different values of the paramenter t. To be precise, we set $\phi = \pi/2k - \pi/k^2$ and we will show that

$$z_e(\phi + \pi/k) = z_h(\phi - \pi/k) \tag{8}$$

and that their moduli is $\cot \pi/k$. We can then appeal to symmetry to cover the other $2k - 1$ middle points. (We should note that we only arrived at equation (8) after a considerable amount of guess-and-check.)

For the left-hand side of equation (8), we use the equation on the left of equation (5), replacing A_k with $\csc \pi/k$ and replacing t with $\phi + \pi/k$, to get

$$\begin{aligned} z_e(\phi + \pi/k) &= e^{i\phi} e^{i\pi/k} \left(\csc \pi/k + e^{i\pi/2} e^{-i\pi/k} e^{i\pi} \right) \\ &= e^{i\phi} \left(e^{i\pi/k} \csc \pi/k + e^{i\pi/2} e^{i\pi} \right) \\ &= e^{i\phi} \left(\frac{\cos \pi/k + i \sin \pi/k}{\sin \pi/k} - i \right) = e^{i\phi} \cot \pi/k. \end{aligned}$$

Likewise, for the right-hand side of equation (8), we use the equation on the right of equation (5) but this time replacing t with $\phi - \pi/k$, to get

$$\begin{aligned} z_h(\phi - \pi/k) &= e^{i\phi} e^{-i\pi/k} \left(\csc \pi/k + e^{-i\pi/2} e^{i\pi/k} e^{i\pi} \right) \\ &= e^{i\phi} \left(e^{-i\pi/k} \csc \pi/k + e^{-i\pi/2} e^{i\pi} \right) \\ &= e^{i\phi} \left(\frac{\cos \pi/k - i \sin \pi/k}{\sin \pi/k} + i \right) = e^{i\phi} \cot \pi/k. \end{aligned}$$

This verifies equation (8), as desired.

It remains to show that the two curves are tangent at that point of equality in equation (8). For this, we recall that the slope of the tangent line to a parametric curve $(x(t), y(t))$ is given by $(dy/dt)/(dx/dt)$. Once more we rely on complex variables to simplify the problem, thanks to the nice property that if $z(t) = x(t) + iy(t)$ then $dx/dt = \text{Re}\, z'(t)$ and $dy/dt = \text{Im}\, z'(t)$, for the real and imaginary parts respectively. Thus, referring back to equation (8), if we can also show that

$$z_e'(\phi + \pi/k) = z_h'(\phi - \pi/k) \tag{9}$$

then this implies the real and the imaginary parts of equation (9) are the same, and so the slopes of the tangent lines are the same at that point of intersection.

For the left-hand side of equation (9), we write $z_e(t) = A_k e^{it} + e^{i(1+k)t}$, so that

$$\begin{aligned} z_e'(t) &= iA_k e^{it} + i(1+k) e^{i(1+k)t} \\ &= ie^{it} \left(A_k + (1+k) e^{ikt} \right) \end{aligned} \tag{10}$$

 © THE MATHEMATICAL ASSOCIATION OF AMERICA

Now, for $t = \phi + \pi/k$ as seen on the left of equation (9), and with $\phi = \pi/2k - \pi/k^2$ as before, we note that

$$kt = (\pi/2 - \pi/k) + \pi$$

and so

$$e^{ikt} = e^{i\pi/2}e^{-i\pi/k}e^{i\pi} = -ie^{-i\pi/k}.$$

This means that equation (10) becomes

$$\begin{aligned} z_e'(\phi + \pi/k) &= ie^{i\phi}e^{i\pi/k}\left(A_k - i(1+k)e^{-i\pi/k}\right) \\ &= ie^{i\phi}\left(A_k e^{i\pi/k} - i(1+k)\right). \end{aligned} \tag{11}$$

Keeping that aside for now, we next turn to the right-hand side of equation (9). We write $z_h(t) = A_k e^{it} + e^{i(1-k)t}$, which means that

$$\begin{aligned} z_h'(t) &= iA_k e^{it} + i(1-k)e^{i(1-k)t} \\ &= ie^{it}\left(A_k + (1-k)e^{-ikt}\right) \end{aligned} \tag{12}$$

Now, for $t = \phi - \pi/k$ as seen on the right of equation (9), and with $\phi = \pi/2k - \pi/k^2$ as before, we note that this time,

$$kt = (\pi/2 - \pi/k) - \pi$$

and so

$$e^{-ikt} = e^{-i\pi/2}e^{i\pi/k}e^{i\pi} = ie^{i\pi/k}.$$

This means that equation (12) becomes

$$\begin{aligned} z_h'(\phi - \pi/k) &= ie^{i\phi}e^{-i\pi/k}\left(A_k + i(1-k)e^{i\pi/k}\right) \\ &= ie^{i\phi}\left(A_k e^{-i\pi/k} + i(1-k)\right). \end{aligned} \tag{13}$$

We now compare equations (11) and (13) to show that they are indeed equal to each other. We start with the expression inside the parenthesis in (11), which is

$$\left(A_k e^{i\pi/k} - i(1+k)\right) = \frac{\cos\pi/k + i\sin\pi/k}{\sin\pi/k} - i(1+k) = \cot\pi/k - ik. \tag{14}$$

Likewise, the expression inside the parenthesis in equation (13) is

$$\left(A_k e^{-i\pi/k} + i(1-k)\right) = \frac{\cos\pi/k - i\sin\pi/k}{\sin\pi/k} + i(1-k) = \cot\pi/k - ik. \tag{15}$$

Since these are the same, then equations (11) and (13) are equal to each other, which establishes the equality in (9), thus showing that the two curves are indeed tangent, as desired. ■

A surprising slope

The highlight in the proof of Theorem 1 was showing that the epitrochoid and hypotrochoid are indeed tangent at the middle point of intersection as seen in Figure 6. This slope exhibits a rather unusual behavior as we increase the value of k, as shown here in Figure 8. Despite the large value of k for the graphs on the right of Figure 8, the

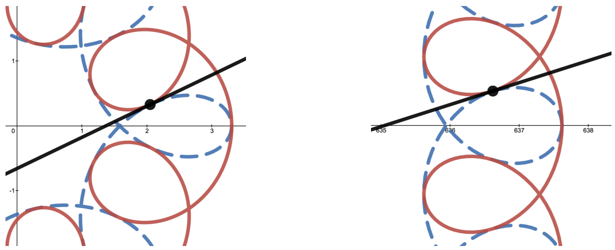

Figure 8. Tangent line at first middle point of intersection for $k = 7$ and $k = 2000$.

teardrop shapes for the epitrochoid (in solid red) and the hypotrochoid (in dashed blue) remain slightly askew, which means the tangent line at that middle point of intersection is not horizontal, nor will it approach horizontal even as k continues to increase. In fact, the limiting value for the slope of this tangent line is rather surprising.

Theorem 2 (Slope Theorem). *For the epitrochoid and hypotrochoid in Theorem 1 with perfect nesting at $A_k = \csc \pi/k$, the slope of the tangent line at the first middle point of intersection above the x-axis approaches $1/\pi$ as $k \to \infty$.*

Proof. Recall from our discussion in the proof of Theorem 1 that the slope of the tangent line is equal to $(dy/dt)/(dx/dt)$ which is equal to $\text{Im } z'(t)/\text{Re } z'(t)$. We look now to equation (11) which gives us the derivative z' of the epitrochoid (and the hypotrochoid as well) at the point of intersection as

$$z' = ie^{i\phi}\left(A_k e^{i\pi/k} - i(1+k)\right),$$

where $\phi = \pi/2k - \pi/k^2$. Thanks to equation (14) this becomes

$$z' = ie^{i\phi}\left(\cot \pi/k - ik\right) = i\left(\cos\phi + i\sin\phi\right)\left(\cot \pi/k - ik\right),$$

and if we multiply this out and simplify then we obtain

$$z' = \left(k\cos\phi - \cot \pi/k \sin\phi\right) + i\left(k\sin\phi + \cot \pi/k \cos\phi\right).$$

Since the slope is $m = \text{Im } z'/\text{Re } z'$, we get

$$m = \frac{k\sin\phi + \cot \pi/k \cos\phi}{k\cos\phi - \cot \pi/k \sin\phi}.$$

We multiply top and bottom by $\sin \pi/k$ to obtain

$$m = \frac{k\sin \pi/k \sin\phi + \cos \pi/k \cos\phi}{k\sin \pi/k \cos\phi - \cos \pi/k \sin\phi}.$$

 © THE MATHEMATICAL ASSOCIATION OF AMERICA

We can now take the limit as $k \to \infty$. Recall that $\phi = \pi/2k - \pi/k^2$, so as $k \to \infty$ then $\phi \to 0$. A simple application of L'Hôpital's rule tells us that $k \sin \pi/k$ approaches π as $k \to \infty$, and so

$$m \to \frac{\pi \sin 0 + \cos 0 \cos 0}{\pi \cos 0 - \cos 0 \sin 0} = \frac{1}{\pi},$$

as desired. ■

Conclusion

As we have seen, the epitrochoid and hypotrochoid reveal some surprising secrets when written in complex variables. We can only wonder what other parametric curves might benefit from a similar treatment.

Summary. Two classic plane curves, the epitrochoid and hypotrochoid, can be placed together in an optimal nested form. We find the appropriate equations by way of complex variables, and we also get a surprising answer for the slope of a particular tangent line.

References

1. Frank A. Farris, *Creating symmetry. The artful mathematics of wallpaper patterns*, Princeton University Press, Princeton, 2015.
2. Alfred Gray, Simon Salamon, and Elsa Abbena, *Modern Differential Geometry of Curves and Surfaces with Mathematica*, Chapman & Hall/CRC, Boca Raton, 2006.
3. J. Dennis Lawrence, *A Catalog of Special Plane Curves*, Dover Publications, New York, 1972.
4. Pradeem Mutalik, Solution: 'Creating Art With Mathematics', *Quanta* (2015). Available at `https://www.quantamagazine.org/solution-creating-art-with-mathematics-20151030/`